PHYSICAL REVIEW B **81**, 035332 (2010)

# Direct measurement of spin dynamics in InAs/GaAs quantum dots using time-resolved resonance fluorescence

C.-Y. Lu,[1,2] Y. Zhao,[1,3] A. N. Vamivakas,[1] C. Matthiesen,[1] S. Fält,[4] A. Badolato,[5] and M. Atatüre[1]
[1]*Cavendish Laboratory, University of Cambridge, JJ Thomson Avenue, Cambridge CB3 0HE, United Kingdom*
[2]*HFNL and Department of Modern Physics, University of Science and Technology of China, Hefei, 230026, China*
[3]*Physikalisches Institut, Ruprecht-Karls-Universität Heidelberg, Philosophenweg 12, Heidelberg 69120, Germany*
[4]*Sol Voltaics AB, Scheelevägen 17, Ideon Science Park, 223 70 Lund, Sweden*
[5]*Department of Physics and Astronomy, University of Rochester, Rochester, New York 14627, USA*
(Received 3 August 2009; revised manuscript received 22 December 2009; published 26 January 2010)

We temporally resolve the resonance fluorescence from an electron spin confined to a single self-assembled quantum dot to measure directly the spin's optical initialization and natural relaxation time scales at 4 K. Our measurements demonstrate that spin initialization occurs on the order of microseconds in the Faraday configuration when a laser resonantly drives the quantum dot transition. We show that the mechanism mediating the optically induced spin-flip changes from electron-nuclei interaction to hole-mixing interaction at 0.6 T external magnetic field. Spin relaxation measurements result in times on the order of milliseconds and suggest that a $B^{-5}$ magnetic field dependence, due to spin-orbit coupling, is sustained all the way down to 2.2 T.

DOI: 10.1103/PhysRevB.81.035332 PACS number(s): 78.67.Hc, 71.35.Pq, 72.25.Rb, 78.55.−m

Single spins confined in semiconductor quantum dots (QDs) interact with nearby charge, spin, and phonon reservoirs in their solid state environment. Signatures of these interactions are imprinted on the spin's dynamics and elucidating the time scales relevant for these couplings is not only interesting from the perspective of mesoscopic physics, but is also important in assessing the potential of a QD electron spin as a qubit in quantum information science.[1] Driven by these motivations a number of studies have begun to quantify both spin relaxation and decoherence time scales.[2–10] For spins confined in optically active semiconductor QDs, there is an additional time scale, namely, the optically induced spin-flip time $T_P$—the time an optical field can recycle a spin-selective dipole transition before a spin-flip event is induced.

Here, we present a direct *n*-shot measurement of spin dynamics in a single self-assembled InAs/GaAs QD due to coupling to both an optical field and the QD environment in the Faraday configuration, as well as originating from internal state mixing mechanisms. We study the explicit dependence of the optically induced spin-flip rate on the properties of the optical field such as Rabi frequency and spectral detuning. We then identify the magnetic field dependent crossover, where the mechanism mediating the spin-flip processes changes from ground-state mixing (due to electron-nuclei coupling) at low magnetic fields to excited-state mixing (due to heavy-light hole coupling). We further demonstrate for the first time that, the natural spin relaxation rate of a single electron, without the influence of an optical field, can vary more than two orders of magnitude following the magnetic field dependence expected from spin-orbit interaction inducing a ground-state spin admixture.[11,12] Finally, we discuss briefly the prospect of time-resolved resonance fluorescence in the context of single-shot read-out of spins in quantum dot systems.

The InAs/GaAs, quantum dots studied in this work were grown by molecular beam epitaxy (MBE) and embedded in a Schottky diode heterostructure; the details of the device can be found in Ref. 13. Such devices allow for deterministic charging of QDs and we consider only the relevant ground and excited states for a single electron charging under magnetic field in the Faraday configuration, which can be understood by the four-level system illustrated in Fig. 1(a). In this representation, the single electron ground states are spin down $|\downarrow\rangle$ or spin up $|\uparrow\rangle$. The two trion excited states consist of an electron singlet and a single hole—depicted as $|\uparrow\downarrow\Uparrow\rangle$ and $|\downarrow\uparrow\Downarrow\rangle$. The magnetic field lifts the zero field degeneracy between the two $X^{1-}$ transitions resulting in a blue (red) shift for the $|\uparrow\rangle\leftrightarrow|\uparrow\downarrow\Uparrow\rangle$ ($|\downarrow\rangle\leftrightarrow|\downarrow\uparrow\Downarrow\rangle$) transition. These transitions are dipole allowed with a spontaneous emission rate of $\sim 2\pi\times 250$ MHz. The $|\downarrow\rangle\leftrightarrow|\uparrow\downarrow\Uparrow\rangle$ transition is normally forbidden due to the conservation of total angular momentum, but the optical selection rules are typically relaxed by both ground and excited-state mixings resulting in a finite relaxation rate $\gamma \ll \Gamma$ on these transitions. As a result, resonant optical excitation of the blue (or red) transition can flip the spin of the ground-state electron—a process we refer to as an optically induced spin flip.[14] The rate $\xi_{\uparrow\downarrow}$ indicates direct spin-flip transitions between the electronic ground states $|\uparrow\rangle\leftrightarrow|\downarrow\rangle$ without the influence of an optical field and can vary orders of magnitude as a function of external parameters such as magnetic and electric field.

For the measurements reported here, the $X^{1-}$ transition is driven by a linearly polarized, frequency and power stabilized, single mode laser. The integrated resonance fluorescence (RF) (Ref. 13 and 15) collected back through the focusing objective passes through a second linear polarizer (orthogonal to the laser polarization) prior to being sent to an avalanche photodiode (APD). In Fig. 1(b), the gray circles fit by the red curve present an exemplary integrated RF spectrum as the laser frequency is swept across the $X^{1-}$ transition. The blue squares in Fig. 1(b) display the background, i.e., the same measurement when the QD transition is Stark-shifted out of resonance. For this measurement, the RF signal-to-background ratio is 18:1 and the signal-to-noise ratio is 160:1 allowing for real-time transition monitoring at higher

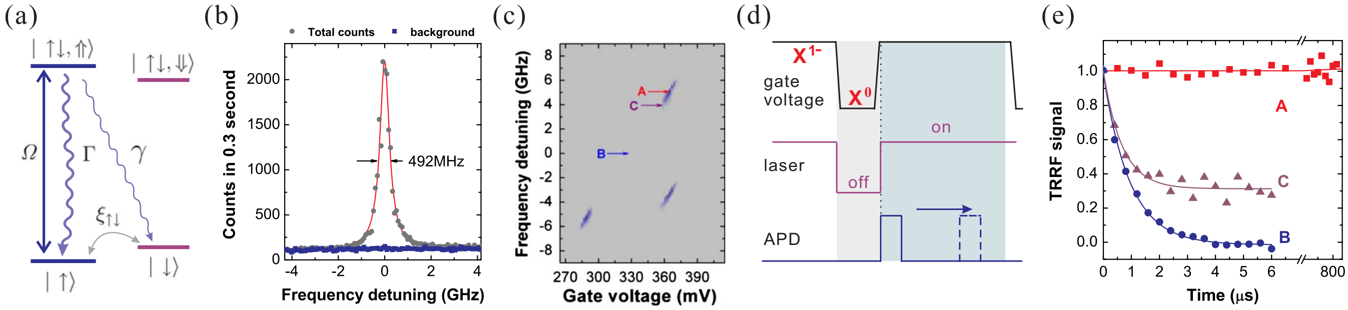

FIG. 1. (Color online) (a) The reduced four-level scheme for a deterministically charged QD. (b) The integrated resonance fluorescence (gray circles) from the $X^{1-}$ transition as a function of laser detuning. The laser power is 0.2 times the spontaneous emission rate and there is no external magnetic field. Each data point corresponds to 300 ms of integration. The blue squares indicate the background level when the transition is far detuned via gate voltage. (c) Two-dimensional DT map under 350 mT magnetic field. (d) One cycle of the protocol for measuring the optically induced spin-flip rate. (e) TRRF signal obtained at the three voltage-frequency conditions highlighted in panel c.

bandwidth in comparison to other optical techniques such as differential transmission (DT).

To investigate the spin dynamics of the confined electron, we apply a magnetic field in the Faraday configuration. Figure 1(c) displays a two-dimensional map of the DT signal of the blue trion transition at 350 mT magnetic field for the full single electron charging plateau. In order to obtain a high precision measure of the optically induced spin-flip time scale $T_P$, we resort to an $n$-shot measurement of the integrated resonance fluorescence spectrum. The details of one measurement protocol cycle are presented in Fig. 1(d), where the first trace indicates the gate voltage controlled charging state of the QD alternating between zero and one excess electron. The second trace indicates the laser amplitude, where the blue-shifted Zeeman transition is excited when the laser is on. The third trace is the APD detection window. We access the time dynamics of the integrated RF spectrum by recording APD counts during a $0.1-2$ $\mu$s time window, which is scanned across the on-window. We repeat this cycle $\sim 10^5$ times for all presented data. Background counts are subtracted for each cycle by far-detuning the transition.

Figure 1(e) presents time-resolved resonance fluorescence (TRRF) measurements for three different combinations of laser frequency and gate voltage highlighted as A, B, and C in Fig. 1(c). The red curve decorated with red squares is from location A at the center of the cotunneling region of the charge-stability plateau. In this region, strong cotunneling with the Fermi sea of the back contact randomizes the confined electron spin and mitigates any spin pumping. Consequently, there is no observable temporal dependence in the emitted photon stream. The disappearance of DT signal at location B was previously used to identify efficient spin pumping resulting from optically induced back-action and the absence of any mechanism leading to appreciable spin heating during the time scales accessible to a DT measurement.[16,17] Nevertheless, the transition still generates a photon stream, like a recycling transition, until a single Stokes photon is emitted.[18] The blue curve decorated with blue circles in Fig. 1(e) presents TRRF data from this location. Here, the transition initially generates the same photon counts but the signal vanishes exponentially within a few microseconds. This time scale is to be interpreted in two ways: from the perspective of state preparation, it takes a few $\mu$s to initialize the electron spin. Alternatively, the transition can be recycled for a few $\mu$s before laser induces an unwanted spin-flip event. Identifying the physical mechanisms that lead to this observation is thus of interest from both perspectives. Finally, the TRRF signal at location C displays the intermediate dynamics: The initial exponential decay due to optical spin pumping is still present, but the signal saturates at a constant value determined by the ratio of spin pumping and cotunneling rates. In this case, the cotunneling rate is $2\pi \times 37$ KHz.

Next, we analyze how the excitation Rabi frequency influences $T_P$ at a fixed magnetic field. The state mixing for fixed magnetic fields yields a branching ratio $\eta$, defined as $\gamma/(\Gamma+\gamma)$,[17] which quantifies the number of photons cycled by the transition before the electron flips its spin. With a fixed branching ratio, the optically induced spin-flip rate is determined by the population in the excited-state $|\uparrow\downarrow\Uparrow\rangle$. Consequently, the spin pumping rate is expected to increase with excitation Rabi frequency until it reaches a saturation value. The inset of Fig. 2(a) displays a log-plot of the TRRF signal obtained for three excitation powers for the gate voltage and laser frequency combination labeled B in Fig. 1(c). The black squares in Fig. 2(a) are the extracted optical spin pumping rates per excitation power. In the limit where the Rabi frequency is much larger than the spontaneous emission rate, the spin-flip rate saturates at a rate of $2\pi \times 200$ KHz.

To elucidate the physical mechanisms which mediate the optical induced spin-flip, we study the magnetic field dependence of $T_P$. The laser power is set well above the saturation power (60 nW) and the gate voltage is fixed at the position equivalent to B in Fig. 1(c). For each magnetic field value, TRRF measurements are performed for a range of laser detunings, where Fig. 2(c) presents an exemplary data and Fig. 2(b) presents the corresponding theoretical behavior. From each data set, one can map out the detuning dependence of the spin pumping rate [Fig. 2(d)] in order to ensure that the magnetic field dependence is obtained on resonance with the transition in the spin-pumping region. Figure 2(e) presents the explicit magnetic field dependence of $T_P$. The fitting curve includes the functional dependence on magnetic field of two dominant mechanisms that mix the spin states coherently, namely, the hyperfine interaction for the electrons and the heavy-light hole mixing for the optically generated tri-

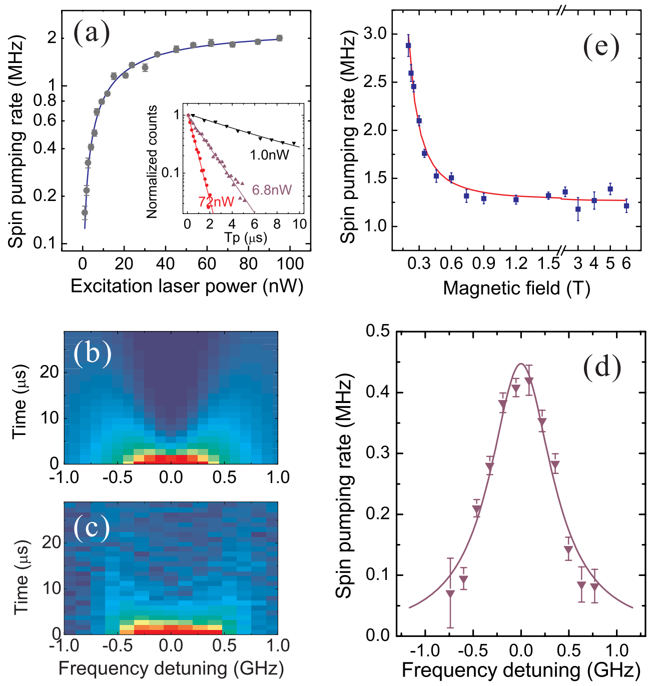

FIG. 2. (Color online) (a) The extracted spin-flip rate from TRRF measurements for a range of laser powers when the laser is resonant with the $X^{1-}$ transition. The saturation power is 18.7 nW. Inset: a log plot of TRRF signal for three laser powers, see supplementary material (Ref. 19) for more raw data. (b) A simulated two-dimensional map of the time-resolved resonance fluorescence for a range of excitation laser frequency detunings and (c) the corresponding experimental data for a fixed laser power of 4 nW. (d) The extracted spin-flip rates as a function of laser detuning, which faithfully map the Lorentzian lineshape of the $X^{1-}$ transition. (e) The magnetic field dependence of the spin-flip rate for a fixed laser power of 60 nW. The lowest magnetic field value of 200 mT is selected to ensure the electronic ground states are split by ~1.5 GHz, which is three times the transition linewidth.

ons. The interaction of the hole spin with the nuclei is neglected here as it is considerably weaker than that of electrons due to its dipolar nature.[20] In the low magnetic field limit, the hyperfine interaction efficiently mediates the spin-flip process and results in a quadratic variation in the spin-flip time with applied external magnetic field according to $(B_N/B_{\text{ext}})^2$, where $B_N$ is the root-mean-square of the random effective field seen by the electron spin due to nuclei. For the QDs considered in this work, this value is typically around 15 mT. Whereas, for magnetic fields beyond 0.6 T, hole spin state mixing in the excited state mediates the spin-flip process and is independent of external magnetic field. This feature is inherent in the matrix material due to band mixing and although it is heavily suppressed in three dimensional quantum confined systems, it is nevertheless finite. The corresponding heavy-light hole-mixing strength is $|\epsilon_{hl}|=2.8\%$ for the QD presented here,[21] which is within the estimated range based on previous reports using differential transmission measurements.[17,22] We do note that the value of hole-mixing strength will vary among QDs due to the shape anisotropy and is related to the large variation in the in-plane hole-spin $g$ factor.

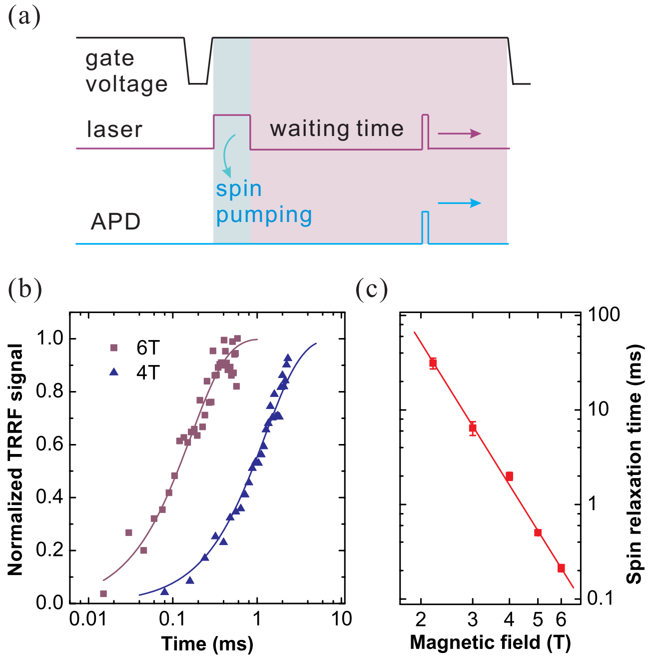

FIG. 3. (Color online) (a) One cycle of the protocol for measuring the spin relaxation time scale. We highlight that at the end of the on-window there is an additional pulse sent to the QD gate (not shown). This artificially but deterministically recycles the QD electron spin and recovers the expected steady-state signal value as determined by the Boltzmann statistics and allows a higher accuracy in theoretical fits. (b) Exemplary TRRF measurements of the spin relaxation time scale for two magnetic field values. (c) The extracted spin relaxation time $T_{\downarrow\uparrow}$ (red squares) as a function of magnetic field. The red curve is the best fit $B^{-5}$ dependence. All TRRF measurements are presented in the supplementary material (Ref. 19), including details on the recycling pulse.

We now present measurements of the natural spin dynamics of a single electron that is not induced by the optical field, i.e., directly between the two ground spin states. The protocol for measuring the spin relaxation is illustrated in Fig. 3(a). The laser is turned on for 50 $\mu$s at the beginning of each cycle, to ensure spin initialization into $|\downarrow\rangle$, then the electron is left in the dark for a waiting time spanning 0–20 ms. The laser is then turned back on for 5 $\mu$s coinciding in time with the detection window. The set of time traces in Fig. 3(b) shows the measured signal recovery for two magnetic field values. Initially, the electron still resides in the dark spin down state $|\downarrow\rangle$ and no photon scattering occurs. As time progresses, and the probability that the electron has flipped its spin orientation increases, the probability to scatter photons also increases. Using the functional dependence of $\rho_{\uparrow\uparrow} \sim a(1-e^{-t/T_{\text{eff}}})$ we extract a corresponding *effective* spin-flip time per magnetic field. Here, $T_{\text{eff}}=T_{\uparrow\downarrow}T_{\downarrow\uparrow}/(T_{\uparrow\downarrow}+T_{\downarrow\uparrow})$ following $(T_{\downarrow\uparrow}/T_{\uparrow\downarrow})=e^{(-g_e\mu_B B/k_B T)}$, where $g_e$ is the electronic $g$ factor taken to be −0.6. The highest measured $T_{\text{eff}}$ of 17.3 ms at 2.2 T corresponds to a $T_{\downarrow\uparrow}$ time of 31.3 ms. The red curve in Fig. 3(c) displays a close agreement with the $B^{-5}$ magnetic field dependence expected for spin relaxation due to single-phonon assisted spin-orbit coupling.[23] This power dependence indicates that the spin-orbit interaction inducing an admixture of electronic ground and excited states is the

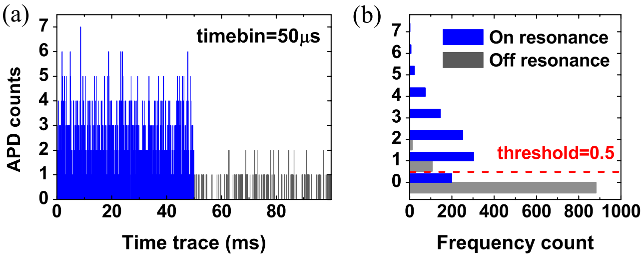

FIG. 4. (Color online) (a) Real-time monitoring of the photon stream scattered from the $X^{1-}$ transition at zero magnetic field (the first 50 ms) and the background counts (the second 50 ms) with a time bin of 50 $\mu$s (left panel), and (b) the corresponding histograms.

dominant mechanism even in the regime of $k_BT>g_e\mu_BB$. This mechanism depends strongly on the electron orbital wave functions and it was recently shown that gate-voltage control of the confinement potential can modify the spin relaxation rate in electrostatic QDs.[10] In self-assembled QDs, a similar correlation between the magnitude and orientation of the X-Y splitting of the neutral exciton states and the single electron spin relaxation rate can be investigated using this technique. The X-Y splitting for the QD studied here is 22 $\mu$eV, twice the mean value of a QD ensemble statistics,[24] so the measured $T_1$ time scales could be even longer for QDs exhibiting vanishingly small XY splitting.

While *n*-shot measurements were employed to record spin initialization and relaxation processes, it is of great interest to quantify the shortest time needed to identify with sufficient fidelity, whether we are probing on resonance or off resonance. In Fig. 4, we present 100 ms worth of real-time RF counts with a 50 $\mu$s time bin; for data on 10 and 30 $\mu$s time bins, we refer the reader to the related supplementary material (Ref. 19) document. The first 50 ms time trace is obtained when the trion transition is resonant with the excitation laser at ~10 times the saturation power. The second 50 ms part is obtained when the transition is far off resonance with the laser dictating the overall background level. The magnetic field is set to zero in order not to obscure the measurements with spin pumping. The read-out error is defined as $\epsilon=\frac{1}{2}(\epsilon_{\text{on}}+\epsilon_{\text{off}})$,[25] where $\epsilon_{\text{on}}$ ($\epsilon_{\text{off}}$) is the fraction of detection attempts where the transition is on (off), but declared to be off (on) since the count is below (above) the set threshold. With a threshold of 0.5, we deduce measurement fidelities $(1-\epsilon)$ of 0.63, 0.77, and 0.84 for the 10, 30, and 50 $\mu$s time bins, respectively. These numbers are satisfactory when compared to spin relaxation time scales and single-shot read-out is in principle possible with sufficient margin with respect to all spin relaxation times of Fig. 3(c). However, for finite magnetic fields the optically induced spin-flip time sets the natural limit for (nondestructive) readout in trionic transition of a single QD configuration, necessitating a measurement time much shorter that 1 $\mu$s. Alternatively, a different QD system demonstrating similar optical measurement and spin relaxation time scales, but not limited by such a short optically induced spin-flip time can be utilized for this purpose. One strong candidate for using TRRF to reveal spin quantum jumps is tunnel-coupled quantum dot pairs,[26,27] where one QD confines a single excess electron and the neighboring QD is in neutral charge configuration. In such a system, the frequency selective probing of the $|\downarrow\rangle\rightarrow|\downarrow\downarrow\Uparrow\rangle$ transition (spectrally shifted from the $|\uparrow\rangle\rightarrow|\uparrow\downarrow\Uparrow\rangle$ transition) with our TRRF technique is expected to yield a significantly reduced rate of spin-flip back-action events (on the order of milliseconds rather than microseconds) and lead to real-time dynamics of electron spin based on the measured time scales reported here.

In summary, we have shown that the time-resolved resonance fluorescence technique presented here allows for accurate and direct measurement of parameters essential to single QD electron spin dynamics, namely, optically induced spin-flip and natural spin relaxation time scales. In addition to demonstrating near-background free QD resonance fluorescence at the $\Omega\approx\Gamma$ excitation regime, we have also shown explicitly the crossover, from hyperfine to hole-mixing, in the mechanism that mediates the optically induced flip of the spin. We have further observed a single magnetic field dependence of the spin relaxation rate down to 2.2 T, which indicates that the dominant reason for spin relaxation is single-phonon assisted spin-orbit coupling mechanism. A natural extension of this work will be looking for correlations between QD confinement anisotropy as signatured in X-Y splitting of the neutral excitons and electron spin relaxation rates. Further, our results indicate that sub-microsecond real-time resolution is necessary for the single-shot measurement of spins using resonant excitation for a single QD configuration, however working with coupled QD systems with our signal-to-noise values is expected to allow real-time monitoring of spin dynamics.

This work was supported by EPSRC under Grant No. EP/G000883/1, QIP IRC, and University of Cambridge. The authors acknowledge fruitful discussions with A. Imamoglu, J. Taylor, L. Jiang, R. B. Liu, and X. Marie.

---

[1] A. Imamoglu, D. D. Awschalom, G. Burkard, D. P. DiVincenzo, D. Loss, M. Sherwin, and A. Small, Phys. Rev. Lett. **83**, 4204 (1999).

[2] J. Elzerman, R. Hanson, L. Van Beveren, B. Witkamp, L. Vandersypen, and A. Kouwenhoven, Nature (London) **430**, 431 (2004).

[3] M. Kroutvar, Y. Ducommun, D. Heiss, M. Bichler, D. Schuh, G. Abstreiter, and J. Finley, Nature (London) **432**, 81 (2004).

[4] R. Hanson, L. H. Willems van Beveren, I. T. Vink, J. M. Elzerman, W. J. M. Naber, F. H. L. Koppens, L. P. Kouwenhoven, and L. M. K. Vandersypen, Phys. Rev. Lett. **94**, 196802 (2005).

[5] J. R. Petta, A. C. Johnson, J. M. Taylor, E. A. Laird, A. Yacoby, M. D. Lukin, C. M. Marcus, M. P. Hanson, and A. C. Gossard, Science **309**, 2180 (2005).

[6] A. Johnson, J. Petta, J. Taylor, A. Yacoby, M. Lukin, C. Marcus, M. Hanson, and A. Gossard, Nature (London) **435**, 925 (2005).

[7] A. Greilich, D. R. Yakovlev, A. Shabaev, Al. L. Efros, I. A. Yugova, R. Oulton, V. Stavarache, D. Reuter, A. Wieck, and M. Bayer, Science **313**, 341 (2006).

[8] D. Press, T. D. Ladd, B. Zhang, and Y. Yamamoto, Nature (London) **456**, 218 (2008).

[9] D. J. Reilly, J. M. Taylor, J. R. Petta, C. M. Marcus, M. P. Hanson, and A. C. Gossard, Science **321**, 817 (2008).

[10] S. Amasha, K. MacLean, I. P. Radu, D. M. Zumbühl, M. A. Kastner, M. P. Hanson, and A. C. Gossard, Phys. Rev. Lett. **100**, 046803 (2008).

[11] A. V. Khaetskii and Y. V. Nazarov, Phys. Rev. B **64**, 125316 (2001).

[12] L. M. Woods, T. L. Reinecke, and Y. Lyanda-Geller, Phys. Rev. B **66**, 161318(R) (2002).

[13] A. N. Vamivakas, Y. Zhao, C.-Y. Lu, and M. Atatüre, Nat. Phys. **5**, 198 (2009).

[14] The relaxation of the selection rules on the $|\downarrow\rangle \leftrightarrow |\uparrow\downarrow\Uparrow\rangle$ transition results in both spontaneous Raman scattering from $|\uparrow\rangle \leftrightarrow |\downarrow\rangle$ and spontaneous emission on the $|\uparrow\downarrow\Uparrow\rangle \leftrightarrow |\downarrow\rangle$ channel when driving $|\uparrow\rangle \leftrightarrow |\uparrow\downarrow\Uparrow\rangle$. Both of these processes flip the ground-state electron spin and we refer to either of these processes as an optically induced spin-flip.

[15] E. B. Flagg, A. Muller, J. W. Robertson, S. Founta, D. G. Deppe, M. Xiao, W. Ma, G. J. Salamo, and C. K. Shih, Nat. Phys. **5**, 203 (2009).

[16] M. Atatüre, J. Dreiser, A. Badolato, A. Hogele, K. Karrai, and A. Imamoglu, Science **312**, 551 (2006).

[17] J. Dreiser, M. Atatüre, C. Galland, T. Müller, A. Badolato, and A. Imamoglu, Phys. Rev. B **77**, 075317 (2008).

[18] G. Fernandez, T. Volz, R. Desbuquois, A. Badolato, and A. Imamoglu, Phys. Rev. Lett. **103**, 087406 (2009).

[19] See supplementary material at http://link.aps.org/supplemental/10.1103/PhysRevB.81.035332.

[20] B. Eble, C. Testelin, P. Desfonds, F. Bernardot, A. Balocchi, T. Amand, A. Miard, A. Lemaitre, X. Marie, and M. Chamarro, Phys. Rev. Lett. **102**, 146601 (2009).

[21] Here, we use the notation, $|\Uparrow\rangle = |+3/2\rangle + \epsilon_+|+1/2\rangle + \epsilon_-|-1/2\rangle$ and $|\epsilon_{hl}| = [|\epsilon_+|^2 + |\epsilon_-|^2]^{1/2}$.

[22] We note that beyond 2 T external magnetic field, TRRF measurements similar to Fig. 2(b) show a dragging of the transition due to dynamical nuclear spin polarization (Refs. 28–30). For the $T_{BA}$ measurements, we operate at nearly zero net nuclear spin polarization and all measurements are performed with constant laser frequency and gate voltage.

[23] A deviation from the $B^{-5}$ to the thermal energy corrected $k_B T B^{-4}$ dependence (Ref. 11) was not observed for the magnetic field range of our experiments.

[24] The deviation from the average value (obtained from measurements on 20 QDs) is likely to result in shorter $T_1$ times due to anisotropy enhanced spin-orbit coupling than similar measurements on a QD ensemble.

[25] A. H. Myerson, D. J. Szwer, S. C. Webster, D. T. C. Allcock, M. J. Curtis, G. Imreh, J. A. Sherman, D. N. Stacey, A. M. Steane, and D. M. Lucas, Phys. Rev. Lett. **100**, 200502 (2008).

[26] L. Robledo, J. Elzerman, G. Jundt, M. Atatüre, A. Hogele, S. Falt, and A. Imamoglue, Science **320**, 772 (2008).

[27] D. Kim, S. E. Economou, S. C. Badescu, M. Scheibner, A. S. Bracker, M. Bashkansky, T. L. Reinecke, and D. Gammon, Phys. Rev. Lett. **101**, 236804 (2008).

[28] C. Latta, A. Hogele, Y. Zhao, A. N. Vamivakas, P. Maletinsky, M. Kroner, J. Dreiser, I. Carusotto, A. Badolato, D. Schuh, W. Wegscheider, M. Atatüre, and A. Imamoglu, Nat. Phys. **5**, 758 (2009).

[29] I. T. Vink, K. C. Nowack, F. H. L. Koppens, J. Danon, Y. V. Nazarov, and L. M. K. Vandersypen, Nat. Phys. **5**, 764 (2009).

[30] X. Xu, W. Yao, B. Sun, D. G. Steel, A. S. Bracker, D. Gammon, and L. J. Sham, Nature (London) **459**, 1105 (2009).